JOURNAL OF PROPULSION AND POWER
Vol. 16, No. 2, March–April 2000

Ignition Characteristics of Plasma Torch for Hydrogen Jet in an Airstream

Kenichi Takita,* Tomokazu Uemoto,† Takahiro Sato,† Yiguang Ju,‡ and Goro Masuya§
Tohoku University, Sendai 980-8579, Japan
and
Katsura Ohwaki¶
Ishikawajima-Harima Heavy Industries Company, Ltd., Yokohama 235-0031, Japan

The ignition characteristics of a plasma torch for a hydrogen jet injected parallel to a subsonic airflow were experimentally studied. The region of the injector position where ignition occurred became gradually narrow with an increase in the distance between the fuel injector and the plasma torch and steeply narrow with an increase in the airflow velocity. This suggests that the ignition limit strongly depends on the penetration height of the plasma torch, which is in inverse proportion to airflow velocity. Nitrogen and oxygen were compared as feed stocks. Results obtained showed no difference in the behavior of the plasma jet itself, the ignition limit, and the flame shape. Calculations of ignition delay time for an H_2/air mixture with the addition of N and O radicals showed the same effectiveness and were found to be superior to the H and the OH radicals. However, the degree of deterioration of an anode nozzle made of copper was more severe for oxygen plasma than for nitrogen.

Nomenclature

A	= emitting area, m^2
C	= constant in Eq. (1)
c	= mole fraction
d_i	= diameter of fuel injector, mm
d_j	= diameter of plasma torch nozzle, mm
H	= penetration height, mm
M	= Mach number
m	= constant in Eq. (1)
U	= airflow velocity, m/s
X, Y, Z	= Cartesian coordinates
ρ	= density, kg/m^3
ϕ	= equivalence ratio

Subscripts

air	= airflow
f	= fuel injection
i	= injection point
PJ	= plasma jet
r	= distance between the fuel injector and gas sampling probe

Introduction

AUTOIGNITION of a fuel injected into a scramjet combustor does not occur at low flight Mach numbers. A plasma torch is considered to be one of most promising igniters for use in such conditions. Thus, it has been investigated and has been used in practice, for instance, in the testing of a subscale scramjet engine model.[1–3]

In previous studies of the plasma torch for use as an igniter in a scramjet combustor,[4–9] various kinds of feed stocks for the torch (H_2, N_2, Ar, Ar/H_2, O_2, and air) were examined from the viewpoints of arc formation, torch stability, requirement for onboard resources, and effectiveness. From the viewpoint of the engine performance, changes in the lowest total temperature of airflow required for ignition in a supersonic flow for different flow rates of feed stock[6] or different numbers of fuel injectors[5,7] have been the main focus. These experiments showed that the ignition characteristics strongly depend on the location of the plasma torch in relation to the fuel injectors.[4,5,7] Therefore, detailed flame structure, flame shape established by the plasma jet, and the relation between the location of a flame and the shape of the plasma jet itself must be clarified to establish the igniter design for supersonic combustors. A few studies have examined the location of the fuel injectors,[4,8,9] but only the streamwise location of the injector was changed (either upstream or downstream of the plasma torch) in those studies. Also, in past research on ignition by a plasma torch, fuel was usually injected perpendicular to the main flow, and parallel injection was scarcely tested. Such injection has some merit, for example, for avoidance of total pressure loss by shock generation or for utilization of the momentum of a fuel flow for the thrust.

In this paper, the ignition characteristics of a plasma torch were investigated by changing the location of the fuel injector in three directions (X, Y, and Z) and by injecting fuel parallel to the main airflow. As a first step for understanding the detailed characteristics of a flame held by a plasma jet in a scramjet combustor, flame shapes, OH emission, temperature, and fuel concentrations around the plasma jet were measured in a subsonic airflow. In addition, the effects of the type of feed stock were investigated experimentally and numerically.

Experimental Apparatus

The test section of the experimental equipment is shown in Fig. 1. It had a 60 × 60 mm square cross section and was 350 mm long. The side walls of the test section were made of Pyrex® glass for optical observation. Subsonic airflow up to 80 m/s ($M_{air} = 0.24$, unit Reynolds number $= 5.3 \times 10^6$ l/m, and the accuracy of the measurement was ±0.2%) was supplied by a turboblower. The pressure and temperature of the airflow were those of the room condition. The boundary-layer thickness of the airflow was about 10 mm at the exit of the test section. Hydrogen was injected parallel to the airflow from a stainless-steel circular tube supported by a strut, the inner diameter d_i of which was 1.45 mm; the flow rate was fixed at 10 l/min (the accuracy of the measurement was ±2%), and the injection velocity

Received 10 May 1998; revision received 5 March 1999; accepted for publication 2 April 1999.

*Research Associate, Department of Aeronautics and Space Engineering; takita@cc.mech.tohoku.ac.jp. Member AIAA.
†Graduate Student, Department of Aeronautics and Space Engineering.
‡Associate Professor, Department of Aeronautics and Space Engineering.
§Professor, Department of Aeronautics and Space Engineering. Member AIAA.
¶Senior Researcher, Advanced Production Engineering Center.

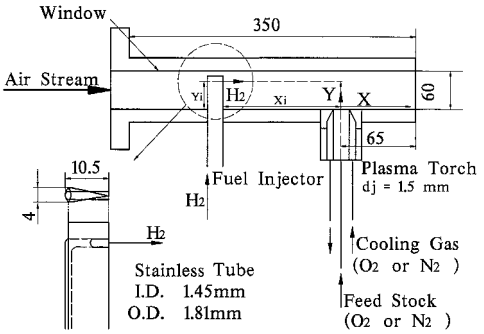

Fig. 1 Schematic of test section.

was about 100 m/s for the experimental conditions. The location of the injector could be moved in the three directions (X, Y, and Z), where X, Y, and Z were the streamwise, lateral, and transverse coordinates, respectively.

The plasma torch used was one slightly improved from that used by Masuya et al.[10] The cathode was made of hafnium to prevent oxidization and deterioration,[6] and the anode was a copper nozzle, the throat diameter d_j of which was 1.5 mm. The diameter of the nozzle at exit was 4 mm, with the opening angle of 60 deg. The throat part was unintegrated from the torch nozzle holder to be easily replaceable when it was damaged. Three kind of gases (N_2, O_2, and air) were used for feed stock. The torch was cooled by the same gas as the feed stock. Electric power for the plasma torch, supplied by a dc power unit, was 1.2 kW for most of the experiments and 1.6 kW for measuring temperature distributions in the Y–Z plane. A high-frequency circuit was attached to the power unit to initiate the plasma arc. The flow rates of the feed stock and coolant were set at 15 l/min and 40 l/min at 288.15 K and 1 atm, respectively. The mass flux ratio of the plasma jet to the airflow changed from 7.9 (U_{air} = 20 m/s) to 2.0 (U_{air} = 80 m/s) for the oxygen plasma and from 6.9 to 1.7 for the nitrogen plasma. Other plasma jet exit conditions were difficult to measure directly because of the high temperature of the plasma, and the main purpose of the study was to investigate the relation between the plasma jet and the flow conditions of the fuel flow and the airflow. Therefore, the injection parameters of the plasma jet were not changed in the experiments.

The torch was installed on the centerline of the bottom wall of the test section, and the plasma jet was injected transversely to the airflow. The ignition of hydrogen fuel was confirmed by the detection of OH emission from hydrogen flame, by the use of a charge-coupled device (CCD) camera with a uv-bandpass filter (central wave length, 303.9 nm; half-value bandwidth, 19.5 nm) and an image intensifier. When OH emission was measured, a rectangular section (40 mm high and 75 mm wide) of a side wall was cut out to detect the emission directly. In addition to OH emission, the sound of combustion could be perceived, which facilitated judgment as to whether ignition occurred or not.

The ignition limit of the fuel injector location was measured for various airflow velocities U_{air}. Intervals of change in the injector location were 20 mm in the X direction, 1 mm in the Y direction, and 5 mm in the Z direction. Moreover, measurements of temperature at the position 30 mm downstream of the plasma torch with a chromel–alumel thermocouple, visualization of the flowfield by schlielen photograph, and gas composition analysis by gas chromatography with a Molecular Sieve 5A column were conducted to enable detailed understanding of the ignition phenomena.

Results and Discussion

Behavior of a Plasma Jet for Different Airflow Velocities

The behavior of a plasma jet without fuel injection was investigated. Oxygen was chosen as the feed stock. The emission from the plasma jet was recorded by the CCD video camera with the OH bandpass filter. Figure 2 shows the shapes of the plasma jet for different airflow velocities. In Fig. 2, the penetration height of the plasma jet decreases, and the jet approaches the wall concomitant with increasing airflow velocity. Figure 3 shows the increase in temperature over the room temperature at 30 mm downstream of the plasma torch. Temperature was not too high due to the mixing of the plasma jet and the airflow at the measurement point. The height of the maximum temperature decreased, and the maximum temperature increased, with increasing airflow velocity. In addition, measurement of temperature in the Y–Z plane showed that the spread of the plasma jet in the Y and Z directions narrowed with the airflow velocity as same as the penetration height. These results indicate that the mixing of the plasma jet and airflow becomes lower as the airflow velocity becomes larger. Two reasons for this suppression of the mixing can be considered. One is the suppression of the mixing in the shear layer between the plasma jet and the airflow by the decrease in the velocity difference. The other reason is that the mixing near the wall was suppressed when the plasma jet was inclined to the wall by the increase in the dynamic pressure of the airflow.

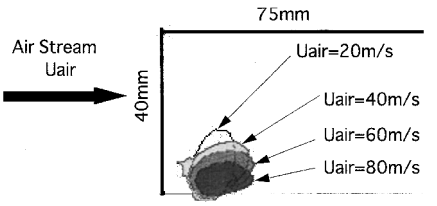

Fig. 2 Shapes of uv emission images of plasma jet for different air velocities (no fuel injection).

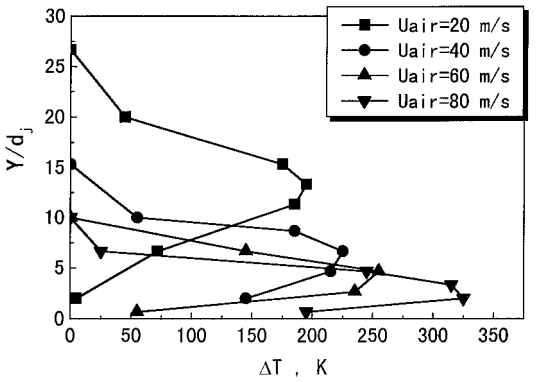

Fig. 3 Temperature rise caused by plasma jet for different airflow velocities at X/d_j = 20 downstream of plasma torch.

Change of Combustion Region with the Fuel Injector Location

The effects of the location of the fuel injector on ignition and on the flame established by the plasma jet were investigated. First, the effect of the height of the fuel injector, Y_i, with constant X_i (X_i/d_j = 30.0), constant Z_i (Z_i/d_j = 0.0), and constant airflow velocity (U_{air} = 20 m/s) were measured.

Figures 4a–4d show the temperature distributions in the Y–Z plane 30 mm downstream of the plasma torch for the case without fuel injection and three cases with fuel injection from different injector heights. The combustion regions are clearly shown in Figs. 4a–4d, though the temperature of combustion gas was decreased by the mixing with the airflow at the measurement location. In Fig. 4a, for the case of no fuel injection, the area of temperature increase was formed only by the plasma jet, and its maximum temperature was about 100 K lower than that of the combustion gas for the case of fuel injection. When a fuel was injected from a low position near the wall (Fig. 4b, Y_i/d_j = 3.3), the combustion region separated into two parts, namely, the region near the wall and the upper part that existed in the range of $15 \leq Y_i/d_j \leq 30$. The combustion region near the wall indicated combustion in the boundary layer of the airflow; the flame sometimes propagated upstream or oscillated, showing the characteristics of a premixed flame. The combustion region in the upper part was produced by combustion of hydrogen convected by the momentum of the plasma jet. These phenomena could also be explained by pictures of OH emission from the hydrogen

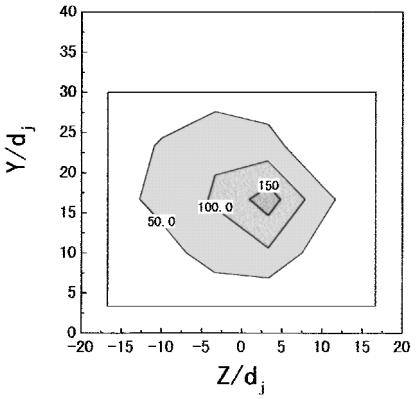

a) No fuel injection

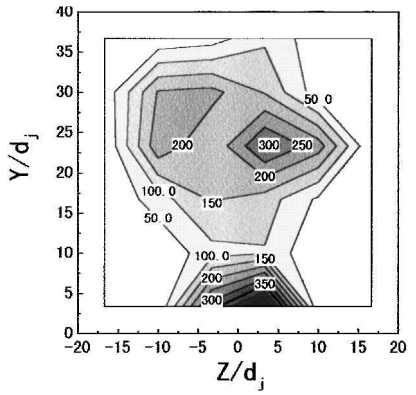

b) $Y_i/d_j = 3.3$

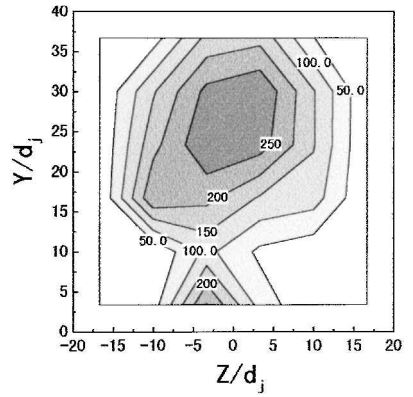

c) $Y_i/d_j = 10.0$

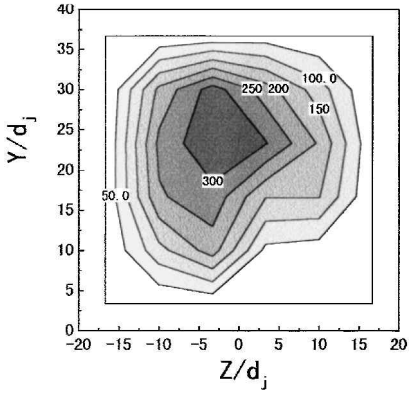

d) $Y_i/d_j = 16.7$

Fig. 4 Temperature contours in the Y–Z plane at $X/d_j = 20$ for U_{air} = 20 m/s, $X_i/d_j = -30$.

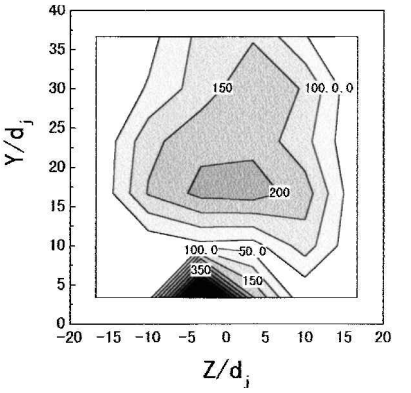

a) $Y_i/d_j = 3.3$

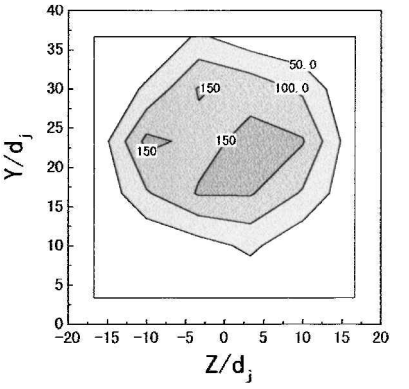

b) $Y_i/d_j = 10.0$

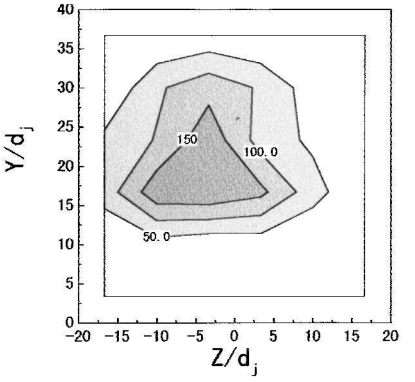

c) $Y_i/d_j = 16.7$

Fig. 5 Temperature contours in the Y–Z plane at $X/d_j = 20$ for U_{air} = 20 m/s, $X_i/d_j = -70$.

flame. In Fig. 4c for $Y_i/d_j = 10.0$, the combustion region in the boundary layer became weaker than that in Fig. 4b, and the combustion region of the upper part was enlarged with an increase in the height of the fuel injector. In Fig. 4d for the case of $Y_i/d_j = 16.7$, the combustion region in the boundary layer disappeared. When the height of the fuel injector became higher than $Y_i/d_j = 16.7$, a stable flame was no longer detected; whereas the intermediate area of the flame detection, where OH and sound emissions were intermittently recognized, appeared for the fuel injection just above and below the height ($Y_i/d_j = 16.7$).

Figures 5a–5c show temperature distributions at the same heights as in Figs. 4b–4d for a different location of the fuel injector ($X_i/d_j = 70.0$). The features of the flame just mentioned were seen for different streamwise locations X_i, although the degree of temperature increase decreased with the increase of the distance between the plasma torch and the fuel injector. However, the dependence of the flame behavior on airflow velocity was apparent. The separation of the combustion region was not observed for high-speed airflow (more than 60 m/s).

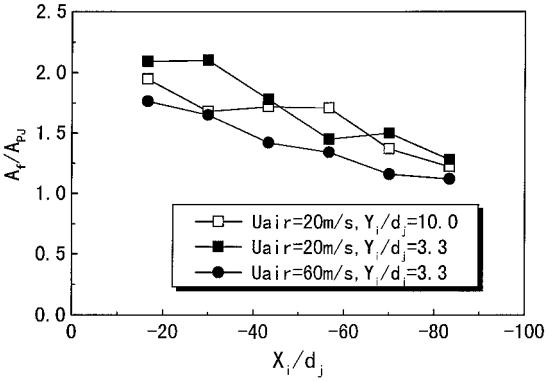

Fig. 6 Change in area ratio of uv emission images with and without fuel injection at different distances between the fuel injector and the plasma torch.

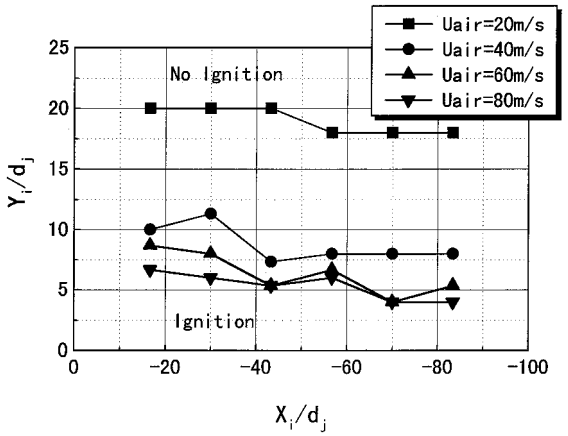

Fig. 7 Ignition limit of the location of the fuel injector (X_i, Y_i) for different airflow velocities.

For the change in the streamwise position of the fuel injector, the image of the uv emission was changed not only in shape but also in area. Therefore, the area of uv emission was analyzed from the video images. First, the emitted region in the X–Y plane was recorded on video tape for the cases with and without fuel injection at the same location of the fuel injector and the same airflow velocity. Next, analog video image data were converted into 8-bit (0–255) gray-scale digital image data and then were two-toned at various threshold values of the gray scale by using software (Photoshop, Adobe Systems). It was confirmed that the ratio of A_f/A_p did not depend on the value of the threshold for the range between 210 and 250. Figure 6 shows the change of A_f/A_p with the streamwise injector location X_i. Each datum in Fig. 6 is an average for 10 pictures taken under the same conditions; the standard deviation is about 3%. The flame area gradually became small with the increase in distance from the fuel injector. This was due to the progress of the diffusion of hydrogen. The same tendency of decreasing flame area for transverse injection was obtained by Kimura et al.[4] They also reported that combustion did not occur due to insufficient mixing of a fuel when the fuel injector was located very close to the plasma torch (the distance was 5 mm). In the experiments reported herein, such a phenomenon was not observed because the minimum distance of the fuel injector from the plasma torch was $16.7d_j$ (25 mm) due to limitations of the experimental apparatus, where mixing of fuel and airflow was sufficient for ignition.

Ignition Limit for the Location of the Fuel Injector

The ignition limit for the location of the fuel injector (X_i, Y_i) where a stable flame could be established was measured for different airflow velocities. In the test section shown in Fig. 1, the flame established by the plasma jet was extinguished if the plasma jet was turned off, which indicated that the ignition limit overlapped the limit of flame holding. Figure 7 shows the ignition limit, not including unstable or discontinuous cases, for different airflow velocities and different locations in the X direction. When the height of the fuel injector became higher than the line of the ignition limit, combustion no longer occurred. As seen in Fig. 7, the height of the fuel injector at the ignition limit was gradually reduced, concurrent with an increase in the distance between the fuel injector and the plasma torch, and steeply reduced with an increase in the airflow velocity. When the distance between the fuel injector and the plasma torch became large, the fuel gradually mixed with the airflow.

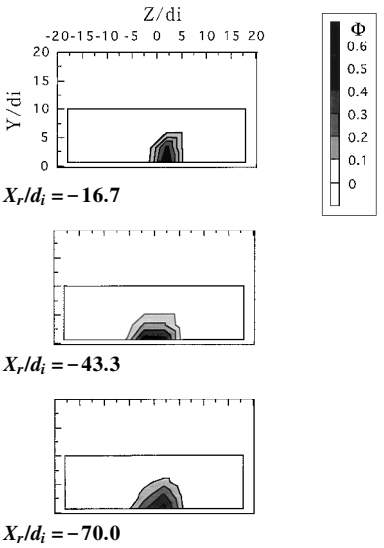

Fig. 8 Contours of equivalence ratio at different distances from the fuel injector ($Y_i/d_j = 3.3$).

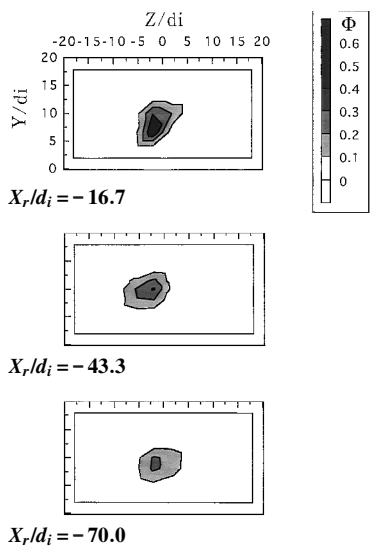

Fig. 9 Contours of equivalence ratio at different distances from the fuel injector ($Y_i/d_j = 10.0$).

To investigate the fuel concentration, gas sampling for the cold flow was conducted in the Y–Z plane. Figure 8 shows distributions of the fuel equivalence ratio at three different distances X_r, when a fuel was injected near the wall ($Y_i/d_j = 3.3$). Figure 9 shows the case where fuel was injected from the mediate height ($Y_i/d_j = 10.0$). The fuel mixture became leaner as X_r increased, but the equivalence ratio at the center of the fuel flow changed little and was greater than that for the flammable limit of the H_2/air mixture, even at $-X_r/d_j = 70$. This was the reason for there being little change in the ignition limit when the fuel injector moved in streamwise direction X. Comparison between Figs. 8 and 9 revealed that the progress in mixing along the X direction was suppressed for the fuel injection near the wall.

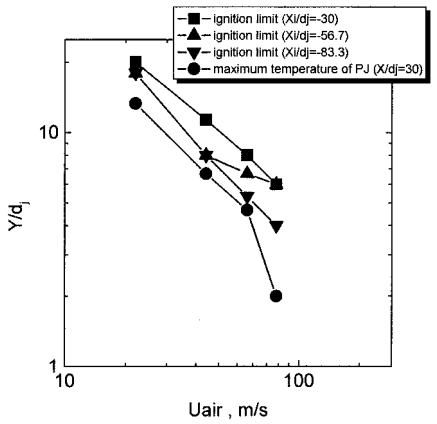

Fig. 10 Dependence of the fuel injector height at ignition limit and penetration height of the plasma jet on airflow velocity.

In contrast to the influence of the streamwise location of the injector, the steep change in the ignition limit was observed with increasing airflow velocity. This result was due to the change in the penetration height of the plasma torch. In Fig. 10, the height of the fuel injector at the ignition limit for three cases of X_i/d_j and the height of the maximum temperature at 30 mm downstream of the plasma torch without fuel injection were plotted for different airflow velocities. Both the height at ignition limit and of the plasma jet decreased linearly with the airflow velocity, and the slope was almost the same on the log scale; thus, it was obvious from this result that the ignition limit depended strongly on the penetration height of the plasma jet.

The penetration height of a jet injected into a subsonic crossflow is related to the dynamic pressure ratio of a jet and an airflow, and the penetration height H_{PJ} was correlated by the following equation[11]:

$$\frac{H_{PJ}}{d_j} = C \cdot \left(\frac{X}{d_j}\right)^m \cdot \left(\frac{\rho_{PJ} U_{PJ}^2}{\rho_{air} U_{air}^2}\right)^{(1-m)/2} \tag{1}$$

In Eq. (1), the velocity and the density of the plasma jet are assumed to be constant for the flow rate and input power of a feed stock, and the Mach number of the airflow is low. Thus, the following relation was obtained:

$$H_{PJ} \propto (1/U_{air})^{1-m} \tag{2}$$

This relation agreed with Fig. 10, although the exponent factor $(1-m)$ obtained from Fig. 10 was about 0.85, which was a little larger than that suggested in Ref. 11, namely, 0.72.

Figure 11 shows schlieren photographs for three cases: in the ignition region ($Y_i/d_j = 10.0$) (Fig. 11a), near the ignition limit ($Y_i/d_j = 20.0$) (Fig. 11b), and out of the ignition limit ($Y_i/d_j = 26.7$) (Fig. 11c). When a fuel was injected from a position higher than that of the ignition limit, the area of interaction between the fuel flow and the plasma jet was very small, as shown in Fig. 11c. It is clear from the comparison of these photographs that high-temperature regions were enlarged by combustion of hydrogen at the upper part of the plasma jet and that ignition occurred when fuel flow collided with a plasma jet. This observation explained the dependence of the ignition limit on penetration height of the plasma jet, as did Fig. 10.

The effect of the location of the fuel injector in the Z direction on the ignition limit is shown in Fig. 12. When $Z_i/d_j = 6.7$, ignition could not occur, even though the ignition limit for the case of $Z_i/d_j = 3.3$ changed little from that for the case of $Z_i/d_j = 0.0$. These results support the hypothesis obtained from examination of the schlielen photographs in Fig. 11, which show that ignition occurred when the fuel flow collided with the plasma jet.

Dependence of Ignition Characteristics on the Kind of Feed Stock

Sato et al.[6] pointed out that oxygen would be better as a feed stock for a plasma torch than argon or an argon/hydrogen mixture from the viewpoint of the total system design of the scramjet engine and the vehicle because oxygen bombs are usually carried in the vehicle,

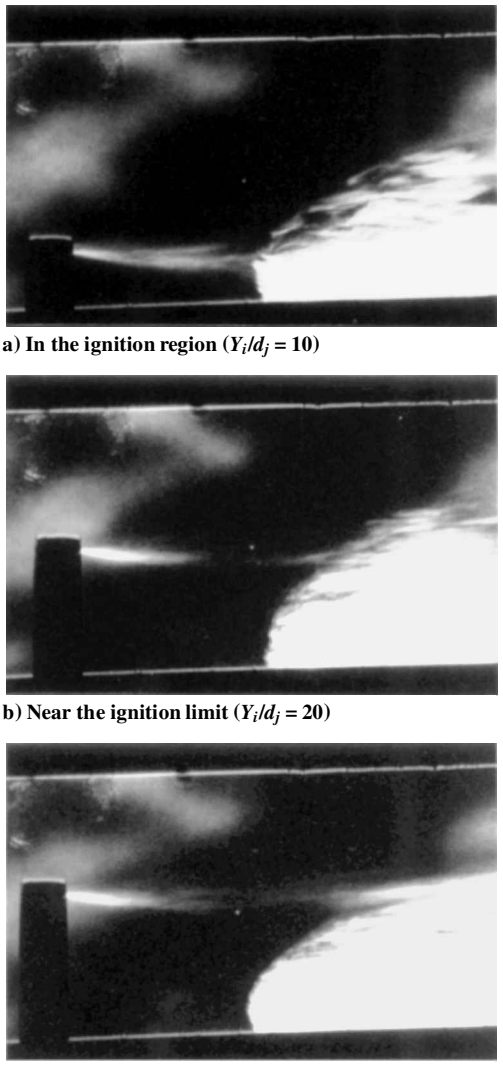

a) In the ignition region ($Y_i/d_j = 10$)

b) Near the ignition limit ($Y_i/d_j = 20$)

c) Out of the ignition limit ($Y_i/d_j = 27$)

Fig. 11 Schlieren photographs for different fuel injector heights ($U_{air} = 20$ m/s).

whereas argon is not carried. Nitrogen might also be carried as the pneumatic control gas. Therefore, nitrogen as a feed stock was compared with oxygen at the same electric power input and flow rates of feed stock and coolant. The shape, penetration height, and uv emission from a N_2 plasma jet without injection of hydrogen showed no differences from those with O_2 plasma. Moreover, the ignition limit of the fuel injector height for N_2 plasma almost coincided with that for O_2 plasma, as seen in Fig. 13. However, the torch nozzle was remarkably less eroded by the N_2 plasma than by the O_2 plasma. In addition, the stability of the N_2 plasma jet was better than that of the O_2 plasma jet. Air plasma showed intermediate results between O_2 and N_2 plasmas.

Calculation of Ignition Delay Time in the Case of the Addition of Radicals

To enable better insight into the preceding results, ignition delay time for an H_2/air mixture with the addition of a small amount of radicals was computed using a perfectly stirred reactor model. Mitani[12] analytically demonstrated that the addition of O radicals was more effective in reducing ignition delay time than addition of OH and H radicals of the same mole fraction, but he did not consider N radicals nor N_2 chemistry. In the calculations, 15 chemical species (H_2, O_2, N_2, H, O, N, OH, H_2O, HO_2, H_2O_2, NO, NO_2, N_2O, NH, and HNO) and 41 elementary reactions, including reactions of NO, a recombination reaction of N atoms, etc., constituted from the tables in Refs. 13 and 14 were used. Figure 14 shows the ignition delay time for the addition of the same mole fraction of O, N, H, OH, and

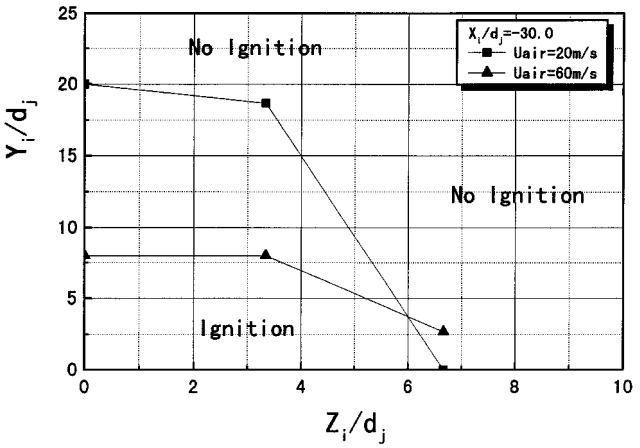

Fig. 12 Ignition limits of fuel injector height in laterally different planes ($X_i/d_j = -30$).

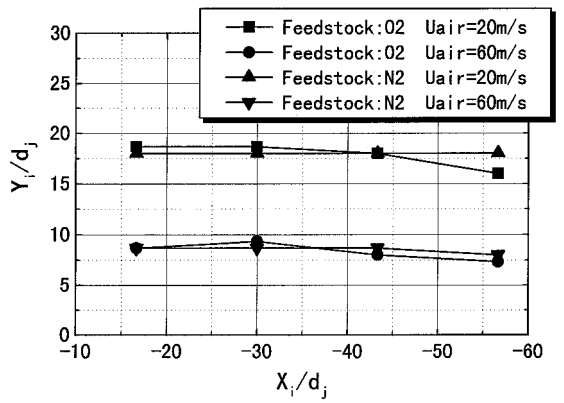

Fig. 13 Height of the fuel injector (X_i, Y_i) at the ignition limit comparing N_2 plasma and O_2 plasma.

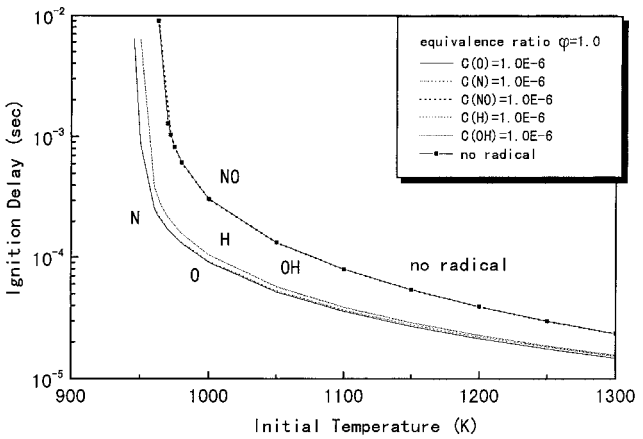

Fig. 14 Computed ignition delay time of the H_2/air mixture with the addition of various radicals: O, N, H, OH, and NO.

NO radicals. It is obvious from Fig. 14 that the N and O radicals showed the same effectiveness in reducing the ignition delay time and were superior to H and OH radicals. Moreover, the NO radicals had a weak effect on reducing ignition delay time in this temperature range. The agreement of the effectiveness between N and O is mainly due to the following rapid reaction:

$$N + O_2 \rightarrow O + NO \quad (3)$$

NO produced by this rapid reaction has little effect on ignition delay as already mentioned. As a result, N and O radicals show the same effect.

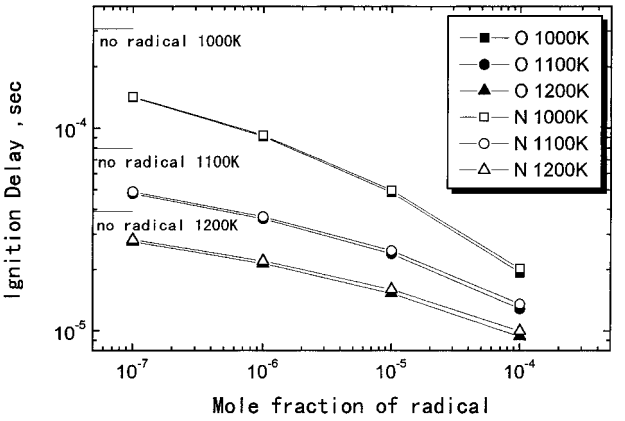

Fig. 15 Effect of radical concentration on reducing ignition delay time.

Figure 15 shows the dependence of the ignition delay time on the mole fractions of the radicals added to the H_2/air mixture. The increase in the mole fraction of radicals shortened the ignition delay time and extended the ignition limit, but there was little difference between N and O. Also, the effect of the equivalence ratio of the H_2/air mixture on ignition delay time was very small and showed little difference between the addition of the O and N radicals.

However, the dissociation rate of O_2 plasma is much larger than that of N_2 plasma for the same electric power if the plasma jet is assumed to be of uniform composition and in equilibrium.[15] Also, the lifetime of N radicals in a low-temperature atmosphere is shorter than that of O radicals. Therefore, a mole fraction of the N radicals must have been different from that of the O radicals in the experiment. In practice, the effect of the difference in dissociation rate between N_2 and O_2 did not appear in the experimental results, indicating that the N_2 plasma jet was as effective as the O_2 plasma jet. A necessary condition for ignition was that a combustible mixture of H_2 and air collided with the plasma jet. The formation of a high-temperature region where radical concentration was also high was a main factor for the ignition process of the plasma jet. In other words, the roles of high temperature and high radical concentration could not be separated. This characteristic may be applied when the plasma jet is located downstream of the fuel injector; in such a case, a flame sticks to the plasma jet. If the plasma torch is located upstream of the fuel injector, the composition of the feed stocks must affect the ignition limit, because, in such a case, the lifetime of the radicals becomes important.

Conclusions

The ignition characteristics of a plasma torch for different locations of the fuel injector, different airflow velocities, and different kinds of a feed stock were investigated experimentally and analytically. The following results were obtained.

1) The ignition limit of the fuel injector height gradually decreased with an increase in the distance between the fuel injector and the plasma torch and steeply decreased with an increase in the airflow velocity. These results suggest that the penetration height of plasma jet strongly influences the ignition limit.

2) The N_2 plasma torch showed the same effectiveness in igniting a hydrogen jet as the O_2 plasma torch in the present experiments, except for much less deterioration of the copper nozzle. As a result, the formation of a high-temperature region played an important role for the plasma jet for the ignition process in the experiment.

3) The effectiveness of a small addition of N radicals and of a small addition of O radicals to the H_2/air mixture in reducing the ignition delay time was almost the same, although they were superior to the addition of H and OH radicals.

4) When fuel was injected near the wall, the combustion regions stabilized by a plasma jet appeared in two parts: One was combustion in the boundary layer of the airflow, which showed the characteristics of a pre-mixed flame, and the other was combustion in the upper

part of the plasma jet, where fuel was convected by the momentum of the plasma jet.

Acknowledgment

The authors wish to thank Katsuyoshi Takahashi and Seiji Yoshida for their support in the experiments and Masao Chiba for his help in the manufacturing of the experimental apparatus.

References

[1]Masuya, G., and Chinzei, N., "Scramjet Engine Tests at Mach 4 and 6," International Union of Theoretical and Applied Mechanics Symposium on Combustion in Supersonic Flows, Kluwer, Dordrecht, 1997, pp. 147–162.

[2]Kanda, T., Hiraiwa, T., Mitani, T., Tomioka, S., and Chinzei, N., "Mach 6 Testing of a Scramjet Engine Model," *Journal of Propulsion and Power*, Vol. 13, No. 4, 1997, pp. 543–551.

[3]Mitani, T., Hiraiwa, T., Sato, S., Tomioka, T., Kanda, T., and Tani, K., "Comparison of Scramjet Engine Performance in Mach 6 Vitiated and Storage-Heated Air," *Journal of Propulsion and Power*, Vol. 13, No. 5, 1997, pp. 635–642.

[4]Kimura, I., Aoki, H., and Kato, M., "The Use of a Plasma Jet for Flame Stabilization and Promotion of Combustion in Supersonic Air Flows," *Combustion and Flame*, Vol. 42, 1981, pp. 297–305.

[5]Wagner, T. C., O'Brien, W. F., Northam, G. B., and Eggers, M., "Plasma Torch Igniter for Scramjets," *Journal of Propulsion and Power*, Vol. 5, No. 5, 1989, pp. 548–554.

[6]Sato, Y., Sayama, M., Ohwaki, K., Masuya, G., Komuro, T., Kudou, K., Murakami, A., Tani, K., Wakamatsu, Y., Kanda, T., Chinzei, N., and Kimura, I., "Effectiveness of Plasma Torches for Ignition and Flameholding in Scramjet," *Journal of Propulsion and Power*, Vol. 8, No. 4, 1992, pp. 883–889.

[7]Masuya, G., Kudou, K., Murakami, A., Komuro, T., Tani, K., Kanda, T., Wakamatsu, Y., Chinzei, N., Sayama, M., Ohwaki, K., and Kimura, I., "Some Governing Parameters of Plasma Torch Igniter/Flameholder in a Scramjet Combustor," *Journal of Propulsion and Power*, Vol. 9, No. 2, 1993, pp. 176–181.

[8]Kato, R., and Kimura, I., "Numerical Simulation of Flame-Stabilization and Combustion Promotion by Plasma Jets in Supersonic Air Streams," *Proceedings of 26th International Symposium on Combustion*, Combustion Inst., Pittsburgh, PA, 1996, pp. 2941–2947.

[9]Nagashima, T., Kitamura, H., and Obata, S., "Supersonic Combustion of Hydrogen in Tandem Transverse Injection with Oxygen Radicals," *Proceedings of Thirteenth International Symposium on Air Breathing Engines*, 1997, pp. 366–373.

[10]Masuya, G., Komuro, T., Murakami, A., Shinozaki, N., Nakamura, A., Murayama, M., and Ohwaki, K., "Ignition and Combustion Performance of Scramjet Combustors with Fuel Injection Struts," *Journal of Propulsion and Power*, Vol. 11, No. 2, 1995, pp. 301–307.

[11]Smith, S. H., and Mungal, M. G., "Mixing, Structure and Scaling of the Jet in Crossflow," *Journal of Fluid Mechanics*, Vol. 357, 1998, pp. 83–122.

[12]Mitani, T., "Ignition Problems in Scramjet Testing," *Combustion and Flame*, Vol. 101, 1995, pp. 347–359.

[13]Sanders, J. P. H., "Nonequilibrium and Differential Diffusion Effects in Turbulent Hydrogen Diffusion Flames," *Journal of Thermophysics and Heat Transfer*, Vol. 11, No. 3, 1997, pp. 384–390.

[14]Miller, J. A., and Bowman, C. T., "Mechanism and Modeling of Nitrogen Chemistry in Combustion," *Progress in Energy and Combustion Science*, Vol. 15, 1989, pp. 287–338.

[15]Kobayashi, K., Mitani, T., and Niioka, T., "Asymptotic Analysis of Plasma Jet Igniter," *Proceedings of 21st International Symposium on Space Technology and Science*, Vol. 1, 1998, pp. 123–128.